Electronic structure of layered perovskite-related Sr1−yLayNbO3.5−x

Christine A. Kuntscher, S. Gerhold, N. Nücker, T. R. Cummins, D.-H. Lu, S. Schuppler, C. S. Gopinath, Frank Lichtenberg, Jochen Mannhart, K.-P. Bohnen

Angaben zur Veröffentlichung / Publication details:

Kuntscher, Christine A., S. Gerhold, N. Nücker, T. R. Cummins, D.-H. Lu, S. Schuppler, C. S. Gopinath, Frank Lichtenberg, Jochen Mannhart, and K.-P. Bohnen. 2000. "Electronic structure of layered perovskite-related Sr1−yLayNbO3.5−x." *Physical Review B* 61 (3): 1876–83. https://doi.org/10.1103/physrevb.61.1876.

Electronic structure of layered perovskite-related $Sr_{1-y}La_yNbO_{3.5-x}$

C. A. Kuntscher, S. Gerhold, N. Nücker, T. R. Cummins,* D.-H. Lu,† S. Schuppler, and C. S. Gopinath‡
Forschungszentrum Karlsruhe, IFP, P.O. Box 3640, D-76021 Karlsruhe, Germany

F. Lichtenberg and J. Mannhart
Experimentalphysik VI, Center for Electronic Correlations and Magnetism, Institute of Physics, University of Augsburg, Universitätsstrasse 1, D-86135 Augsburg, Germany

K.-P. Bohnen
Forschungszentrum Karlsruhe, IFP, P.O. Box 3640, D-76021 Karlsruhe, Germany

(Received 1 June 1999)

The electronic properties and the crystal structure of layered perovskite-related niobates $Sr_{1-y}La_yNbO_{3.5-x}$ can be tuned by gradually changing the oxygen stoichiometry. We have studied the electronic structure of this series in detail by angle-integrated and angle-resolved (ARPES) photoemission and x-ray absorption (NEXAFS) on $SrNbO_{3.45}$ and $La_{0.1}Sr_{0.9}NbO_{3.39}$ single crystals. ARPES shows a one-dimensional dispersion and a purely one-dimensional Fermi surface with a nesting vector $2k_F = 0.56$ Å^{-1}. A strongly anisotropic electronic character appears in polarization-dependent O 1*s* NEXAFS as well. Local-density approximation (LDA) band-structure calculations support this dispersion behavior of the lowest-lying conduction band and find additional Fermi surface sheets with a more two-dimensional character.

I. INTRODUCTION

Perovskite-derived oxidic materials with layered structure have been receiving special interest in the past few years, often fueled by the quest for new cuprate or copper-free oxide superconductors. A recently synthesized perovskite-related family[1] with the formal composition $ABO_{3.5-x}$, where B is a transition metal (TM) and A is a large pre-TM element, typically an alkaline earth or rare earth, exhibits complex but systematic superlattice structures depending on oxygen content. The interplay with the associated electronic structure is, however, not clear at this time. Members of this family that have been grown in single crystals include conducting layered alkaline earth niobates and rare-earth titanates.[2–4] These compounds form the homologous series $A_{n+1}B_{n+1}O_{3n+5}$ and are derived from the three-dimensional (3D) perovskite ABO_3 by ''cutting'' the edges of the BO_6 octahedra parallel to the (110) plane and inserting additional oxygen. This is related to the well-known Ruddlesden-Popper scheme[5] where a (100) cut accompanied by the insertion of AO leads to the series $A_{n+2}B_{n+1}O_{3n+4}$. Starting from the ferroelectric insulating compound $SrNbO_{3.5}$,[6,7] the electronic properties of the series $SrNbO_{3.5-x}$ can be gradually tuned by decreasing the oxygen content, involving structural changes. A second doping channel consists of partial substitution of divalent strontium by higher-valent atoms like lanthanum. Both channels cause electron doping and leave niobium in a mixed-valent state (Nb^{5+}, Nb^{4+}). In the range $0<x<0.08$, well-ordered intergrowth takes place between insulating ($n=3$) and conducting ($n=4$) subunits, resulting in new superlattices where the stacking sequence of the subunits is determined by the oxygen stoichiometry. For example, $SrNbO_{3.45}$ consists of alternating $n=3$ and $n=4$ slabs. This compound exhibits activated electrical transport with activation energies in the meV range, both parallel ($\rho_\parallel$) and perpendicular ($\rho_\perp$) to the cleavage plane, and the anisotropy ratio $\rho_\perp/\rho_\parallel$ falls within the interval 10^2 to 10^3, depending on temperature.[2]

The rich array of possible superstructures calls for a systematic exploration of the electronic properties and of how they are affected by the two doping channels mentioned above. In this paper, we present a detailed study of the electronic properties of two representative compounds of the series $Sr_{1-y}La_yNbO_{3.5-x}$–$SrNbO_{3.45}$ (Ref. 8) and $La_{0.1}Sr_{0.9}NbO_{3.39}$–using angle-integrated and angle-resolved photoemission (UPS, ARPES) as well as near-edge x-ray absorption (NEXAFS) spectroscopy. The ARPES results suggest a one-dimensional metallic character for both compounds, which will be discussed on the basis of band- structure calculations in the local-density approximation.

II. EXPERIMENT

$SrNbO_{3.45}$ and $La_{0.1}Sr_{0.9}NbO_{3.39}$ single crystals were grown by a floating zone melting process under Ar atmosphere. Details on the preparation process and the characterization of the crystals in terms of thermogravimetric analysis, electrical transport properties, and magnetic susceptibility can be found in Ref. 2. By powder x-ray diffraction (XRD) and high-resolution transmission electron microscopy[3] (HRTEM) the room temperature crystal structure of the Sr-Nb-O $n=3$ and $n=4$ members was determined to have orthorhombic symmetry, with lattice parameters estimated to $a \approx 3.9$ Å and $b \approx 5.5$ Å. A structural feature common to all members of the series $Sr_{1-y}La_yNbO_{3.5-x}$ are corner-sharing NbO_6 octahedra whose Nb-O base planes are (100) oriented and that are connected continuously along the *a* axis through their apical sites (Fig. 1). Along the *c* direction, the sequence of the octahedra is broken up periodically by Sr interlayers, effectively producing *a*-*b* slabs that are $(n+1)$ octahedra wide. In the case of $SrNbO_{3.45}$, HRTEM diffraction patterns exhibit a periodicity in the layer-stacking *c* direction with a

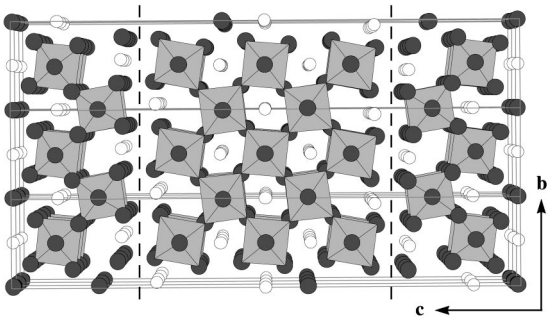

FIG. 1. Projection along the a axis of the $SrNbO_{3.4}$ ($n=4$) crystal structure (shown are three unit cells along b). Note the a-b slabs with a width of $n+1$ NbO_6 octahedra. The Nb atoms (hidden) occupy the central sites of the octahedra, and the O atoms (grey circles) occupy the octahedral vertices. The Sr atoms are represented by white circles. The bold dashed lines indicate the most likely position of the (001) cleavage plane.

wavelength of ≈ 59 Å, consistent with a stacking sequence –[3–4–3–4]– of individual $n=3$ and $n=4$ slabs per unit cell. Indeed, HRTEM images show this sequence to be perfectly ordered.[3] A detailed XRD analysis[9] for the composition $SrNbO_{3.4}$ revealed a unit cell with $a=3.995(2)$ Å, $b=5.674(2)$ Å, and $c=32.456(5)$ Å in the space group Pnnm. These values are taken as an approximation for the crystal parameters of $La_{0.1}Sr_{0.9}NbO_{3.39}$. The crystals typically have a size of $2\times4\times1$ mm^3 and cleave perpendicular to the layer-stacking direction c, presumably along the Sr interlayers between two adjacent slabs.

Angle-integrated (UPS) and angle-resolved (ARPES) photoemission measurements were performed with a discharge lamp using the He I α line at 21.22 eV and the Ne I line at 16.85 eV, respectively. Contributions from satellite lines (16.67 eV for Ne and 23.09 eV for He) were subtracted for the spectra presented. For ARPES, the energy resolution was set to 50 meV and 90 (100) meV as determined by the Fermi edge of freshly evaporated gold films at 17 K. Better resolution had to be sacrificed in exchange for a reasonable count rate. The angular acceptance of the hemispherical analyzer (VSW HA54) amounts to $\pm1°$, corresponding to a $\mathbf{k}$ resolution of about 0.06 Å^{-1}. Sample surfaces suitable for photoemission studies were prepared by cleaving the crystals *in situ* prior to the measurement, exposing an (001) surface. Surface quality was checked regularly by comparing characteristic valence-band features. With the base pressure at $<3\times10^{-11}$ mbar, ARPES data could be recorded up to about 18 hours after cleaving without observing any degradation of the spectra. The orientation of the samples was determined to within $\pm1°$ by low-energy electron diffraction (LEED). The sharp, bright spots observed indicate high surface quality. Data for photoemission in the constant-initial-state (CIS) mode were recorded at beamline 6.2 at the Synchrotron Radiation Source, Daresbury Laboratory (UK), using light with $h\nu=33\ldots44$ eV and an angle-integrating VSW 100 mm hemispherical analyzer.

Polarization-dependent O 1s near-edge x-ray absorption (NEXAFS) measurements were performed at beamline U4B of the National Synchrotron Light Source, Brookhaven National Laboratory, with the energy resolution set to ≈210 meV. The spectra were recorded in the nonsurface

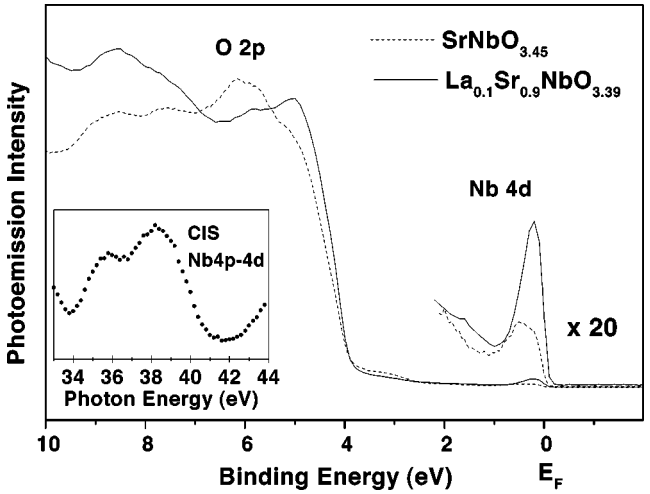

FIG. 2. UPS spectra for $SrNbO_{3.45}$ and $La_{0.1}Sr_{0.9}NbO_{3.39}$ taken at room temperature with $h\nu=21.22$ eV. Note that the intensity of the near-E_F feature is increased for the latter by a factor of ≈3. Inset: CIS spectrum of the near-E_F peak at 0.6 eV for $SrNbO_{3.45}$. The enhancement of the photoemission signal around $h\nu=38$ eV (Nb $4p\rightarrow4d$ threshold) suggests this peak to be Nb $4d$ derived.

sensitive fluorescence yield mode, which gives a probing depth on the order of 1000 Å, and were corrected for saturation and self-absorption effects.[10] For energy calibration, total electron yield data of NiO were taken simultaneously and referred to a NiO standard[11] from electron energy-loss spectroscopy, resulting in an absolute energy calibration of about 0.1 eV. The present data are corrected for the energy-dependent incident photon flux monitored by the current from a gold mesh, and normalized to tabulated atomic absorption cross sections[12] at about 70 eV above the absorption edge.

All spectra shown were recorded at room temperature except for ARPES, where the temperature was set to 150 K and 100 K for $SrNbO_{3.45}$ and $La_{0.1}Sr_{0.9}NbO_{3.39}$, respectively. For the compound $SrNbO_{3.45}$, below 150 K the resistivity increases substantially and leads to charging effects on the crystal surface, as seen in spectra measured at 100 K. No charging effects were observed at 100 K for the La-doped system due to its better electrical conductivity.

III. RESULTS

By UPS, we have probed the valence band of the present niobate compounds. The UPS spectra of Fig. 2 exhibit a main valence band ranging from about 4 to 10 eV. In addition, there is a small but well-defined peak close to the Fermi level, E_F, whose tail extends up to E_F. This feature is presumed to be mainly Nb $4d$ derived. For $La_{0.1}Sr_{0.9}NbO_{3.39}$, the intensity ratio R of this near-E_F feature relative to the main valence band has increased by a factor of 3 ($R\approx3\%$) compared to $SrNbO_{3.45}$ ($R\approx1\%$). In a simple ionic picture, the Nb atoms in $SrNbO_{3.45}$ and $La_{0.1}Sr_{0.9}NbO_{3.39}$ are in a mixed valent state (Nb^{5+}, Nb^{4+}) with nominally 0.1 and 0.32 Nb $4d$ electrons per formula unit. This enhanced number of Nb $4d$ electrons in $La_{0.1}Sr_{0.9}NbO_{3.39}$ agrees well with the observed increase in R, supporting in turn the assumption

above that the near-E_F spectral weight is Nb $4d$ derived. The presence of some Nb^{4+} in the samples is also illustrated in x-ray photoemission spectra (not shown) where the main Nb $3d$ core-level peaks due to Nb^{5+} ions exhibit small shoulders at the lower binding-energy side.[13]

The Nb $4d$ character is supported by the CIS result for $SrNbO_{3.45}$ shown in the inset of Fig. 2, where the photoemission intensity of the near-E_F feature at 0.6 eV was tracked while tuning the incident photon energy in the range 33 to 44 eV: The photoemission signal exhibits an enhancement around the Nb $4p \rightarrow 4d$ threshold energy at 38 eV due to constructive interference of the direct photoemission channel $4p^6 4d^n + h\nu \rightarrow 4p^6 4d^{n-1} + e$ with the indirect channel $4p^6 4d^n + h\nu \rightarrow 4p^5 4d^{n+1} \rightarrow 4p^6 4d^{n-1} + e$. In a similar photoemission and x-ray absorption study on the related compound $La_xSr_{1-x}TiO_3$, Fujimori *et al.*[14] were able to assign Ti $3d$ character to the spectral weight within about 4 eV below E_F, in close analogy with our results. Moreover, they assign O $2p$ character to the valence band that they find between 4 and 9 eV; a similar assignment is expected to hold for $SrNbO_{3.5-x}$ as well.

ARPES was applied to resolve distinct bands within the near-E_F feature and to explore their dispersion relations. Photoelectron energy distribution curves (EDC's) are measured versus momentum $\mathbf{k}_\parallel = (k_x, k_y)$ within the surface Brillouin zone (SBZ). The components of $\mathbf{k}_\parallel$ are related to the electron emission angles θ, ϕ given in the figures via $k_x = (\sqrt{2mE_{kin}}/\hbar) \cdot \sin\theta$ and $k_y = (\sqrt{2mE_{kin}}/\hbar) \cdot \sin\phi$. As the compounds under investigation have a layered structure, no dispersion along the direction $k_\perp$ perpendicular to the cleavage plane is expected. Figure 3 shows EDC's along the high-symmetry lines $\bar{\Gamma}$-$\bar{X}$ and $\bar{\Gamma}$-$\bar{Y}$ for $La_{0.1}Sr_{0.9}NbO_{3.39}$ with an energy resolution of 90 meV [panels (a) and (c)]; additionally, panel (b) contains EDC's taken along $\bar{\Gamma}$-$\bar{X}$ with 50 meV resolution. At the $\bar{\Gamma}$ point, two bands are observed with binding energies of about 600 and 300 meV. The latter band exhibits no significant dispersion along $\bar{\Gamma}$-$\bar{X}$. In contrast, starting from $\bar{\Gamma}$ and moving up to larger angles θ the other peak disperses strongly towards E_F, piles up at $(\theta,\phi) = (10°,0°)$, and has lost the majority of its intensity at $(\theta,\phi) = (12°,0°)$. Using the higher-resolution data the Fermi surface (FS) crossing is determined to occur at $(\theta,\phi) \approx (10°,0°)$. Moving to higher angles θ causes the peak to reappear at $(\theta,\phi) = (16°,0°)$ and to disperse away from the Fermi level, indicating a crossing between $(\theta,\phi) = (14°,0°)$ and $(\theta,\phi) = (16°,0°)$. At the position $(\theta,\phi) = (-10°,0°)$ the peak piles up again near E_F and looks similar to the one at $(\theta,\phi) = (10°,0°)$ suggesting a further FS crossing. In the perpendicular direction $\bar{\Gamma}$-$\bar{Y}$ both bands show no dispersion. ARPES on $SrNbO_{3.45}$ (Fig. 4) also finds two bands, whose dispersion behavior is very similar to the one for $La_{0.1}Sr_{0.9}NbO_{3.39}$. All this suggests that both materials should have metallic character, albeit only in one dimension.

The EDC's about the $\bar{X}$ point resemble very closely those about the $\bar{\Gamma}$ point, with respect to all parameters including binding energy at the bottom of the band, dispersion, and intensity. This is not at all required by the crystal symmetry

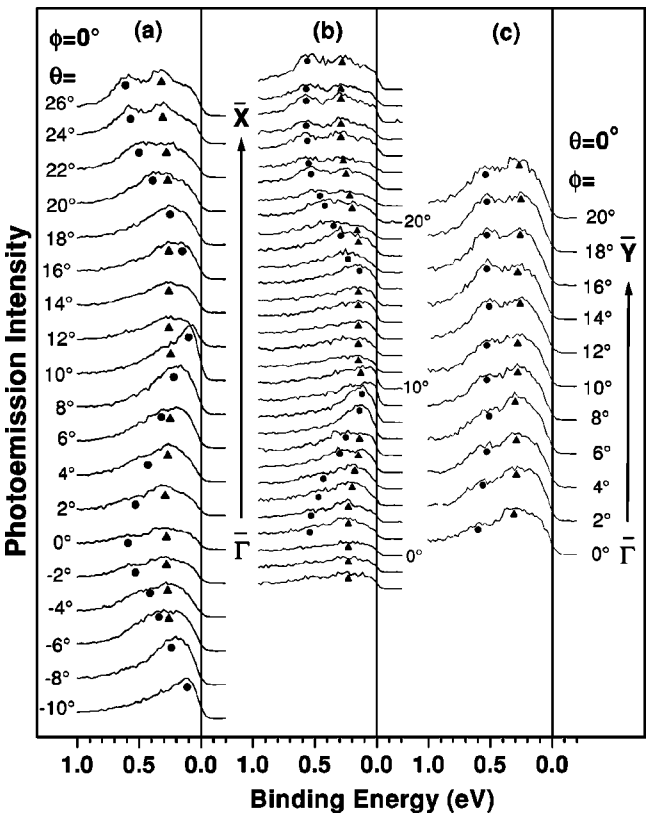

FIG. 3. ARPES for $La_{0.1}Sr_{0.9}NbO_{3.39}$ at $T = 100$ K using $h\nu = 16.85$ eV photons. Spectra taken along $\bar{\Gamma}$-$\bar{X}$($\bar{\Gamma}'$) with (a) 90 meV and (b) 50 meV energy resolution and along (c) $\bar{\Gamma}$-$\bar{Y}$ with 90 meV energy resolution.

and is, in fact, indicative of a reconstruction of some sort. Indeed, such a reconstruction is observed by LEED on the cleaved surface (Fig. 5): A reproducible spot with lower intensity can clearly be seen along the a^* direction of the reciprocal lattice between any two adjacent bright spots of the main pattern. The corresponding (2×1) reconstruction of the (001) plane leads to a folding down of the BZ, causing the $\bar{\Gamma}$ point of the reconstructed zone, called $\bar{\Gamma}'$, to be located right on top of the $\bar{X}$ point of the unreconstructed zone. Very recent neutron scattering experiments[15] show this reconstruction to be a bulk, not a surface effect.

The complete (001) Fermi surface (FS) of $La_{0.1}Sr_{0.9}NbO_{3.39}$ was mapped with an energy resolution of 90 meV and is shown in Fig. 6. The points within the SBZ where EDC's were recorded are indicated by circles. They were chosen to lie on lines parallel to $\bar{\Gamma}$-$\bar{X}$, where the strongly dispersive band is observed [Fig. 3(a)]. For all these cuts the FS crossing of the dispersing band occurs at $k_x \approx 0.28$ Å^{-1}. Obviously, the FS consists of two straight lines parallel to the $\bar{\Gamma}$-$\bar{Y}$ direction, separated by a ''nesting vector'' $2k_F = 0.56 \pm 0.06$ Å^{-1}; in other words, the FS as observed in ARPES has a purely *one-dimensional* character.

The occupied part of the strongly dispersing band covers $\approx$36% of the SBZ (shaded area in Fig. 6) and thus corresponds to 0.72 electrons. Taking into account the second, non-dispersing band, which also lies close to but completely below E_F, one arrives with ARPES at a total of 2.72 elec-

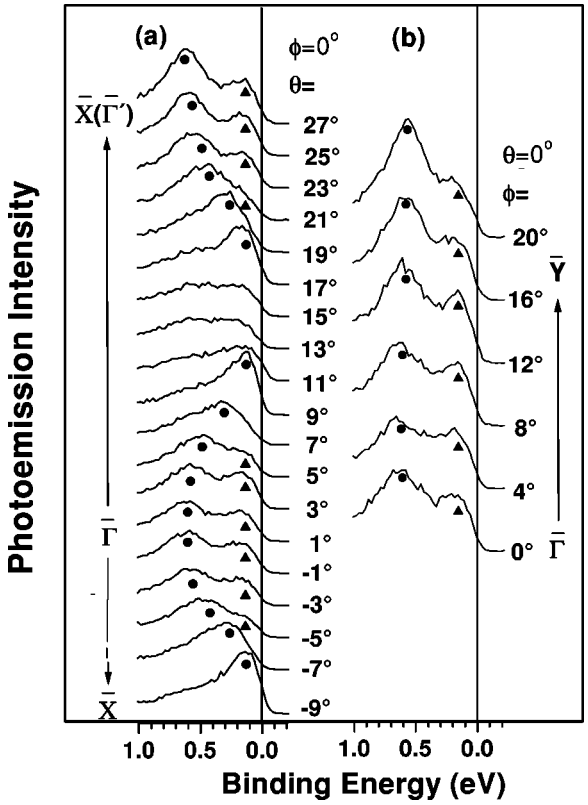

FIG. 4. ARPES for $SrNbO_{3.45}$ at $T=150$ K using $h\nu=16.85$ eV photons; energy resolution 100 meV. Spectra taken along the (a) $\bar{\Gamma}$-$\bar{X}$($\bar{\Gamma}'$) and (b) $\bar{\Gamma}$-$\bar{Y}$ high-symmetry lines.

trons filling the near-E_F Nb $4d$ density of states.[16] On the other hand, the 0.32 Nb $4d$ electrons per formula unit from the ionic picture correspond to 3.2 electrons per unit cell occupying the Nb $4d$ level. The discrepancy to the electron count derived from ARPES hints that there may be additional bands very close to E_F, possibly forming small electron pockets around $\bar{\Gamma}$, which are not recorded by ARPES.

With near-edge x-ray absorption (NEXAFS), one can probe the unoccupied density of states (DOS) near E_F; more

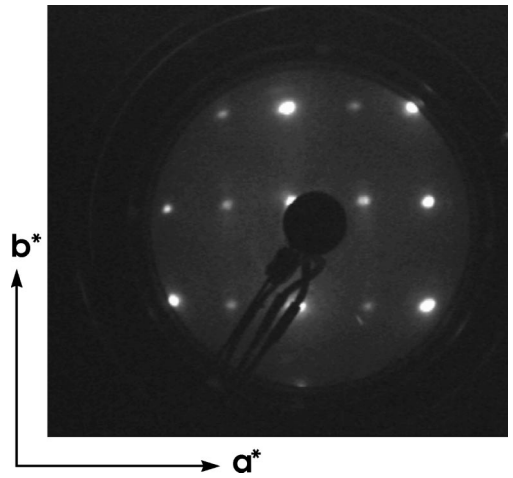

FIG. 5. Typical LEED pattern of $La_{0.1}Sr_{0.9}NbO_{3.39}$ and $SrNbO_{3.45}$ single crystals. Along the a^* direction, (2×1) superstructure reflections are observed.

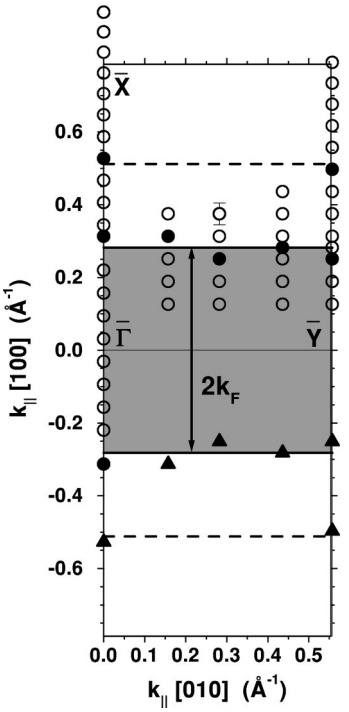

FIG. 6. Measured FS of $La_{0.1}Sr_{0.9}NbO_{3.39}$: ARPES data were taken at points (k_x,k_y) denoted by circles. The FS crossings (filled circles) lie on a straight line. Crossing points obtained by symmetry are indicated by filled triangles. The FS has one-dimensional character with nesting vector $2k_F=0.56\pm0.06$ Å^{-1}. The shaded area indicates the occupied part of the strongly dispersing band. The (2×1) superstructure produces a replica of the FS (dashed-straight line).

specifically: a *partial* DOS, as dipole selection rules allow transitions from, e.g., O $1s$ states only into states with O $2p$ character. It is also a *local* DOS as it probes only a region with sufficient overlap with the core level under consideration. In the niobate compounds studied here, O $2p$ states are hybridized with Nb $4d$ states, and following our UPS results, a considerable Nb contribution is expected near E_F. The O $1s$ NEXAFS data presented may therefore serve as an illustration of the unoccupied Nb $4d$ DOS as well.[17] Furthermore, the symmetry of the final states can be probed by choosing different orientations of the polarization vector **E** relative to the crystal axes a, b, and c. The NEXAFS results for $La_{0.1}Sr_{0.9}NbO_{3.39}$ and $SrNbO_{3.45}$ are presented in Fig. 7 for the polarization vector **E** oriented parallel to the crystal axes. All spectra could be measured at appropriately cut or cleaved surfaces, except for the $La_{0.1}Sr_{0.9}NbO_{3.39}$ $\mathbf{E}\|c$ spectrum, which is extrapolated from data measured in 60° grazing incidence.

All O $1s$ NEXAFS spectra exhibit a peak in the energy range 530–532 eV, immediately above threshold, followed by a marked intensity valley. For both $SrNbO_{3.45}$ and $La_{0.1}Sr_{0.9}NbO_{3.39}$ the spectrum for $\mathbf{E}\|a$ stands out: The onset of the first peak is shifted by about 0.3 eV towards lower photon energies and its intensity is enhanced by 30% to 40% over the other directions. The origin of this first peak can be understood in a simple way in terms of molecular orbitals of a single NbO_6 octahedron; as the Nb $4d$ levels are occupied by at most one electron the first peak in NEXAFS would correspond to transitions into the Nb$4d$-O$2p\pi^*$ antibonding

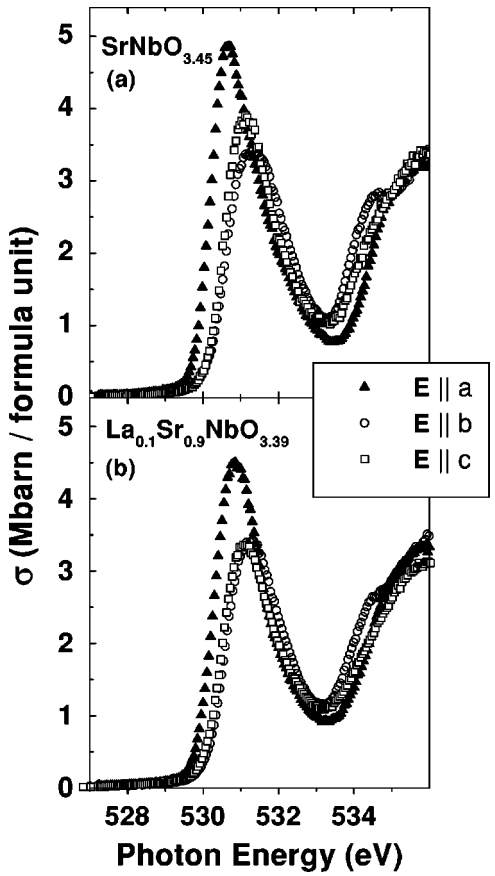

FIG. 7. O 1*s* NEXAFS spectra for $La_{0.1}Sr_{0.9}NbO_{3.39}$ and $SrNbO_{3.45}$ with polarization direction **E** along the crystal axes *a*, *b*, and *c*.

orbitals. For in-plane polarization in O 1*s* NEXAFS, transitions occur from the O 1*s* core level into empty O 2*p* orbitals lying within the plane, while for $\mathbf{E}\|a$ such transitions are into O 2*p* orbitals oriented perpendicular to the Nb-O base plane. Again, looking at just one NbO_6 octahedron, molecular orbitals involving all 6 O atoms will contribute to $\mathbf{E}\|b,c$ spectra, while for $\mathbf{E}\|a$, the 4 O atoms of the base plane contribute, each involving hybridization with the t_{2g} subset of *d* states. This multitude of contributions would require some knowledge of their relative energies to be interpreted unanimously, and thus site-specific NEXAFS measurements are less straightforward here than, e.g., for cuprates with their predominantly σ bond character at E_F. Moreover, there is a large number of inequivalent O and Nb sites within a unit cell due to the various degrees of canting and distortion of the NbO_6 octahedra (see Fig. 1), which further complicates a detailed interpretation of the NEXAFS features. More insight would be offered by comparison with NEXAFS cross sections calculated from band structure; such calculations will be presented separately.[18]

Here, we summarize that the pronounced polarization dependence observed indicates directly a strong anisotropy of the electronic structure, similar to the one already observed by ARPES. Furthermore, it clearly shows that the anisotropic character is indeed a bulk property.

IV. DISCUSSION

The observation of this pronounced one-dimensional (1D) electronic structure in ARPES is quite unexpected, especially as the spatial structure can, by construction of the homologous series and by the cleaving behavior, most naturally be described as ''layered'' or 2D. Furthermore, the 1D Fermi surface suggests a one-dimensional metallic character, and therefore seems to stand in contrast to the macroscopically observed semiconducting behavior.[2] The latter point does not, however, constitute a discrepancy as the in-plane resistivity measured in Ref. 2 most probably has both *a* and *b* contributions.

To explain the former point, on the other hand, would seem to require revising the picture of a layered, essentially 2D crystal structure applied so far which may be oversimplified. An equally valid description of the $n=3$ and $n=4$ subunits considers them as being built up by linear chains of NbO_6 octahedra joined through their apical sites and aligned along the crystallographic *a* axis, while the correlation between the chains may be confined to within the respective subunit (cf. Fig. 1). Although being somewhat naive in itself, this picture makes plausible a spatial structure with quasi-1D character which could explain the anisotropic electronic properties and furthermore the one-dimensional dispersion observed.

To shed some more light on these questions, we performed band-structure calculations in the local-density approximation (LDA) and within the pseudopotential framework for the composition $SrNbO_{3.40}$ with a pure $n=4$ crystal structure. The experimentally determined atomic positions taken from Ref. 9 were used with no relaxation allowed in the calculations. However, we could show that relaxation forces are small. The electronic wave functions are represented in terms of a mixed basis set consisting of a linear combination of atomic orbitals and plane waves. The localized functions consist of one *s* and three *p* functions per oxygen site, three *p* functions per strontium site, and of five *d* functions per niobium site. These functions are atomic pseudo-wave functions that are cut off at a radius R_c where they are joined smoothly to a set of plane waves. In the present case, plane waves up to a kinetic energy of 16 Ry have been taken into account. Details of the method can be found in Ref. 19. Norm conserving pseudopotentials of Hamann-Schlüter-Chiang type were utilized, and for the exchange and correlation potential, the Hedin-Lundqvist approximation was used. For oxygen the 2*s* and 2*p*, for strontium the 4*p* and 5*s*, and for niobium the 4*d* and 5*s* electrons have been treated as valence electrons. Brillouin zone integrations are carried out for 280 points in the zone. From these calculations we find that the system turns out to be a metal; the number of states immediately below E_F is, however, very small. When going further down below E_F, this small near-E_F DOS is followed by an energy gap. These findings have been confirmed in the meantime by an LMTO band structure calculation which will be published elsewhere.[18] To be able to draw comparisons with our ARPES data of $La_{0.1}Sr_{0.9}NbO_{3.39}$, containing about 0.1 electron per formula unit more than the structure for which the calculations were performed, one may apply a rigid band model to the LDA results as a first approximation.[21] The filling of the LDA total density of states (TDOS) of $SrNbO_{3.40}$ with additional electrons, corresponding to 10% La doping, would cause a shift of the Fermi level by 80 meV.

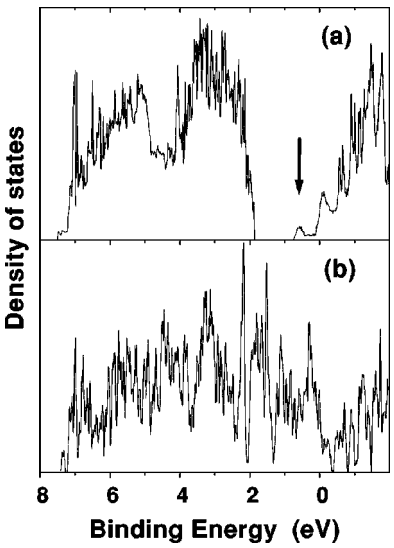

FIG. 8. LDA TDOS of $SrNbO_{3.40}$ with (a) ''real'' (experimental) and (b) ''ideal'' (artificial) crystal structure. The former exhibits a small density of states (indicated by an arrow) right below E_F, followed by an energy gap of width >1 eV. For (b), this gap is filled up completely by additional O $2p$-derived states.

The LDA TDOS and the LDA dispersion relations along the three high-symmetry lines Γ-X, Γ-Y, and Γ-Z are presented in Fig. 8 (a) and Fig. 9, respectively, for the composition $SrNbO_{3.40}$. The LDA TDOS closely resembles our UPS results of Fig. 2: The valence band is located between 7.5 and 2 eV binding energy; the calculations show it to have mainly O $2p$ character. It is separated from the conduction band (whose character is mainly Nb $4d$, consistent with our assignment above) by an energy gap with a width of about 1 eV. Right below E_F, there is a small density of states concentrated around ≈ 580 meV binding energy (indicated by an arrow), to which altogether seven bands contribute. Along the Γ-Z high-symmetry line the LDA band structure exhibits very little dispersion for all bands. At the Γ point, there are two degenerate bands with binding energy of ≈ 750 meV and a number of bands with complicated dispersion located right at E_F. The two degenerate bands do not show any discernible dispersion along Γ-Y, whereas along Γ-X they

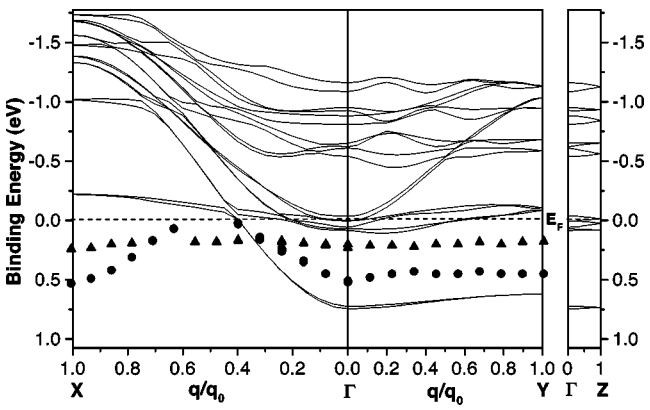

FIG. 9. LDA band dispersion for $SrNbO_{3.40}$ along the high-symmetry lines Γ-X, Γ-Y, and Γ-Z. Symbols: ARPES results for $La_{0.1}Sr_{0.9}NbO_{3.39}$ (Fig. 3), referred to a Fermi level 80 meV above the E_F indicated in the figure to account for La doping (see text).

are dispersing strongly and cross E_F. Our ARPES results for $La_{0.1}Sr_{0.9}NbO_{3.39}$ are included in the figure; to account for the extra La doping the experimental binding energies are referred to a virtual E_F located 80 meV above $E=0$. The general agreement between LDA and ARPES is very good regarding the 1D dispersion behavior of the lowest band, and the experimental effective mass of the lowest band along Γ-X, $m^*/m_0=0.56$, is only slightly enhanced over the LDA value ($m^*/m_0=0.47$). The agreement between experiment and theory is less good around E_F, where LDA exhibits additional bands at E_F with some dispersion both along Γ-X and Γ-Y. According to LDA, altogether seven bands cross E_F along Γ-X and therefore contribute to the Fermi surface of the material. As pointed out above, the electron count derived from ARPES indicates the existence of further FS sheets. Also, when going back to Fig. 3 and inspecting again the spectra in the middle panel, taken at high resolution, one does find some small indication for additional structure at E_F. Still, this evidence is less than conclusive; possible causes for the lack of experimental observation include interference effects in the photoemission process.

An important question to be asked when studying transition-metal compounds concerns the role of correlation. The observation above that the effective-mass enhancement for the lowest-lying conduction band is only small points to a minor role of correlation effects in the niobates under study here. This view is further supported by recalling that correlation effects are most significant for $3d$ TMs like Ti, V, and Cu with their fairly compact $3d$ orbitals; they are reduced for TMs with more extended $4d$ and $5d$ orbitals.[20] In the same vein, we note that for $SrNbO_{3.45}$ and $Sr_{0.9}La_{0.1}NbO_{3.39}$, the nominal $4d$ electron count is very low: just 0.1 and 0.32, respectively, making charge fluctuations that lead to more than single orbital occupancy and to correlation effects quite unlikely. All this, together with the fact that the ARPES results presented above are quite similar for both materials indicates that the features observed in the present study are not strongly influenced by correlation.

Returning to the problem of what could cause the lowest-lying conduction band to be 1D in character, we have calculated the partial density of states to find out which atoms within the unit cell contribute to the near-E_F feature and to what extent. The result is illustrated in Fig. 10 superimposed on the a-projection of the $n=4$ crystal structure. Only the Nb contributions are depicted as all other contributions remain far smaller. Within the five corner-sharing octahedra wide slabs (see also Fig. 1), the Nb partial DOS is maximum for the atoms located in the middle of the slabs and decreases substantially towards the edges. This might be linked to characteristic distortions of the NbO_6 octahedra observed by x-ray diffraction:[9] The Nb atoms with maximum contribution are sitting right in the center of the NbO_6 octahedra, whereas the ones contributing considerably less are displaced up to 13% (0.25 Å) from the central octahedral position. As a crude test if this kind of distortion can decrease the Nb contribution to such an extent the LDA TDOS was calculated for the ''ideal'' $SrNbO_{3.40}$ crystal structure, i.e., a modified structure where the Nb displacements have been artificially removed. As shown in Fig. 8(b), this spatial correction causes the energy gap to be filled up completely by additional, mainly O $2p$-derived states. Also, the dispersion of

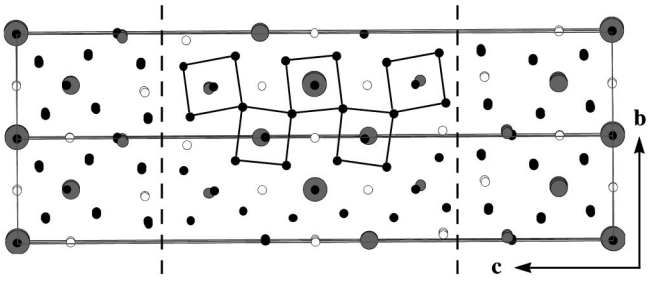

FIG. 10. Illustration of the LDA partial density of states in terms of the projection of the $n=4$ crystal structure along the a axis: Nb atoms are represented by filled grey circles, O atoms by filled black circles, and Sr atoms by open circles. The diameter of the grey circles reflects the strength of Nb contribution to the near-E_F feature of the LDA total density of states, according to LDA. The contribution of the Nb atoms in the middle of the slabs is maximum.

the bands around E_F (not shown) is now considerably more 2D in character, indicating a close connection of the 1D FS observed in ARPES with characteristic distortions of the NbO_6 octahedra. Again, the results are fully consistent with LMTO findings[18] for the same ''ideal'' structure.

There are further important implications raised by the purely 1D FS as seen in ARPES, with a nesting vector that is constant over the whole SBZ, as it looks almost like a textbook example of a 1D system that should be extremely susceptible to structural instabilities with wavelength $1/(2k_F)$ accompanied by a charge density wave.[22] In fact, many photoemission experiments on both organic and inorganic quasi-1D metals have shown a suppression of spectral weight right at E_F,[23] effectively obscuring any observation of a 1D FS. Possible explanations range from the simple CDW or Peierls picture just mentioned[24] to strong CDW fluctuations, resulting in a pseudogap for temperatures above the Peierls transition, and to strong electron-electron interaction. In the latter case, such systems can no longer be regarded as Fermi liquids but instead have to be interpreted in the framework of a Luttinger liquid,[25] with underlying charge-spin separation. In the light of all this, one is indeed led to wonder why in the present case, such an unusual 1D FS is observable at all!

Regarding the Peierls and CDW framework, it is conceivable that the presence of the additional electron pockets around $\bar{\Gamma}$ as seen in LDA has a stabilizing effect for the system as a whole against the $1/(2k_F)$ distortion, maybe simply due to an overcompensation of the energy gain for the lowest-lying band by a concurrent increase in energy for the other bands. In this case one could, in a manner of speaking, call this a ''frustrated'' Peierls behavior. Furthermore, it should be borne in mind that for the niobate compounds considered here, the number of Nb $4d$ electrons may be too small to cause significant correlation effects (cf. our remarks above). It may, therefore, not be sufficient for inducing a Luttinger liquid behavior.

V. SUMMARY

By photoemission (UPS, CIS, ARPES) and x-ray absorption (NEXAFS) measurements both the occupied and unoccupied electronic structure of layered perovskite-related $SrNbO_{3.45}$ and $La_{0.1}Sr_{0.9}NbO_{3.39}$ single crystals have been examined. In ARPES, an anisotropic electronic structure was found with one-dimensional dispersion along $\bar{\Gamma}$-$\bar{X}$ and the highly unusual observation of a Fermi surface with one-dimensional character. The anisotropic electronic character is consistent with polarization-dependent O $1s$ NEXAFS results. LDA band-structure calculations for $SrNbO_{3.40}$ show considerable agreement with ARPES in terms of a quasi-one-dimensional electronic structure. Very close to E_F, LDA predicts a variety of further bands, which are not observed in ARPES. The results presented here clearly call for further studies of the interplay between the spatial and the electronic structure in this type of perovskite-related materials. Specifically, having found a purely one-dimensional sheet within the full Fermi surface, it is highly interesting to see how it evolves upon further doping, and thus gain additional insight into the delicate balance between spatial distortions and the dimensional character of bands.

ACKNOWLEDGMENTS

We are grateful to H. Winter for many fruitful discussions and for performing the TDOS integration of Fig. 8(a). Research was carried out in part at the National Synchrotron Light Source at Brookhaven National Laboratory, which is supported by the U.S. Department of Energy, Division of Material Sciences and Division of Chemical Sciences, under Contract No. DE-AC02-98CH10886. Beamtime at Synchrotron Radiation Source, Daresbury Laboratory, Warrington (UK) is also gratefully acknowledged. We thank S. Stadler, J. Freeland, Y. U. Idzerda, J.-H. Park, W. Flavell, M. Roper, and D. Teehan for valuable and generous experimental assistance. We are grateful to L. Pintschovius and M. Braden for making available their neutron scattering results. D.-H. Lu and C. S. Gopinath thank the VW Foundation and the von-Humboldt Foundation, respectively, for financial support during their stay at Karlsruhe. This work was supported by the BMBF (Project No. 13N6918/1).

*Present address: Lawrence Livermore National Laboratory, Livermore, California 94550.

†Present address: Stanford University, Stanford, California 94305.

‡Present address: University of California Riverside, Department of Chemistry, Riverside, California 92521.

[1] J. G. Bednorz, K. H. Wachtmann, R. Broom, and D. Ariosa, in *High-T_c Superconductivity 1996: Ten Years after the Discovery*, Vol. 343 of *NATO Advanced Study Institute, Series E: Applied Sciences,* edited by E. Kaldis, E. Liarokapis, and K. A. Müller (Kluwer, Dordrecht, 1996), p. 95.

[2] F. Lichtenberg, T. Williams, A. Reller, D. Widmer, and J. G. Bednorz, Z. Phys. B **84**, 369 (1991).

[3] T. Williams, F. Lichtenberg, C. Widmer, J. G. Bednorz, and A. Reller, J. Solid State Chem. **103**, 375 (1993).

[4] T. Williams, H. Schmalle, A. Reller, F. Lichtenberg, D. Widmer, and G. Bednorz, J. Solid State Chem. **93**, 534 (1991).

[5] S. N. Ruddlesden and P. Popper, Acta Crystallogr. **10**, 538 (1957); **11**, 54 (1958).

[6] S. Nanamatsu, M. Kimura, K. Doi, and M. Takahashi, J. Phys. Soc. Jpn. **30**, 300 (1971).

[7] It is worth noting that the ferroelectric transition temperature for $SrNbO_{3.5}$, 1342 °C [see M. E. Lines and A. M. Glass, *Principles and Applications of Ferroelectrics and Related Materials* (Clarendon Press, Oxford, 1977)], is among the highest ones reported for any ferroelectric. This makes such compounds interesting candidates for ferroelectric data storage devices.

[8] First ARPES results of $SrNbO_{3.45}$ have been published previously in D. H. Lu, C. S. Gopinath, M. Schmidt, T. R. Cummins, N. Nücker, S. Schuppler, and F. Lichtenberg, Physica C **282-287**, 995 (1997).

[9] H. W. Schmalle *et al.*, Acta Crystallogr., Sect. C: Cryst. Struct. Commun. **51**, 1243 (1995); S. C. Abrahams, H. W. Schmalle, T. Williams, A. Reller, F. Lichtenberg, D. Widmer, J. G. Bednorz, R. Spreiter, Ch. Bosshard, and P. Günter, Acta Crystallogr., Sect. B: Struct. Sci. **54**, 399 (1998).

[10] L. Tröger, D. Arvanitis, K. Baberschke, H. Michaelis, U. Grimm, and E. Zschech, Phys. Rev. B **46**, 3283 (1992); S. Eisebitt, T. Böske, J.-E. Rubensson, and W. Eberhardt, *ibid.* **47**, 14 103 (1993).

[11] M. Knupfer *et al.* (private communication).

[12] W. V. Veigele, *Handbook of Spectroscopy* (CRC Press, Cleveland, 1974), Vol. 1, p. 28ff.

[13] F. Lichtenberg, D. Widmer, J. G. Bednorz, T. Williams, and A. Reller, Z. Phys. B **82**, 211 (1991).

[14] A. Fujimori, I. Hase, M. Nakamura, H. Namatame, Y. Fujishima, Y. Tokura, M. Abbate, F. M. F. de Groot, M. T. Czyzyk, J. C. Fuggle, O. Strebel, F. Lopez, M. Domke, and G. Kaindl, Phys. Rev. B **46**, 9841 (1992).

[15] L. Pintschovius (private communication).

[16] This simple calculation assumes nondegeneracy of the observed bands.

[17] Note that although Nb $L_{2,3}$ or Nb $M_{2,3}$ NEXAFS could, in principle, provide *direct* information on the unoccupied Nb $4d$ DOS at E_F, one would gain very little as the associated core-hole lifetime broadenings are 1.7 and 2.1 eV, respectively, in effect washing out any details of the electronic structure. Besides, the $M_{2,3}$ edges for elements with $Z>30$ are known to be fairly weak. See M. O. Krause, J. H. Oliver, J. Phys. Chem. Ref. Data **8**, 329 (1979); N. Mårtensson and R. Nyholm, Phys. Rev. B **24**, 7121 (1981); C. C. Ahn and O. L. Krivanek, *EELS Atlas* (HREM Facility, Arizona State University, Tempe, 1983).

[18] H. Winter, S. Schuppler, and C. A. Kuntscher, J. Phys. Condens. Matter (to be published).

[19] C. Elsasser, N. Takeuchi, K. M. Ho, C. T. Chan, P. Braun, and M. Fähnle, J. Phys.: Condens. Matter **2**, 4371 (1990).

[20] This is illustrated in, e.g., A. Fujimori, I. Hase, H. Namatame, Y. Fujishima, Y. Tokura, H. Eisaki, S. Uchida, K. Takegahara, and F. M. F. de Groot, Phys. Rev. Lett. **69**, 1796 (1992), where for the $5d^1$ TM compound ReO_3, no correlation effects are observed in UPS, in contrast to $3d^1$ TM compounds like $SrVO_3$ and $YTiO_3$.

[21] For oxygen doping, the rigid band assumption would be much less justified due to the structural changes associated with the intercalation; this was shown theoretically for the related family $Sr_{1-y}La_yTiO_{3-\delta}$. See N. Shanthi and D. D. Sarma, Phys. Rev. B **57**, 2153 (1998).

[22] One should not confuse such a ''Peierls'' distortion, however, with the distortion of NbO_6 octahedra across a given slab, which is caused by their inequivalent environments. Also, it cannot be related to the 2×1 reconstruction observed in LEED and ARPES, as the corresponding wave vector has a very different magnitude.

[23] For an overview see G. Margaritondo, Proc. SPIE **2696**, 488 (1996), and references therein; M. Grioni, H. Berger, M. Garnier, F. Bommeli, L. Degiorgi, and C. Schlenker, Phys. Scr. **T66**, 172 (1996); F. Zwick, D. Jérome, G. Margaritondo, M. Onellion, J. Voit, and M. Grioni, Phys. Rev. Lett. **81**, 2974 (1998); J. D. Denlinger, G.-H. Gweon, J. W. Allen, C. G. Olson, J. Marcus, C. Schlenker, and L.-S. Hsu, *ibid.* **82**, 2540 (1999). The suppression of spectral weight at E_F for $Li_{0.9}Mo_6O_{17}$ observed in ARPES by Denlinger *et al.*, see above, has very recently been called into question by a new ARPES study: J. Xue *et al.*, Phys. Rev. Lett. **83**, 1235 (1999).

[24] R. E. Peierls, *Quantum Theory of Solids* (Oxford University Press, London, 1955).

[25] F. D. M. Haldane, J. Phys. C **14**, 2585 (1981).